Coordination Chemistry Reviews, 109 (1991) 181–205
Elsevier Science Publishers B.V., Amsterdam

MULTIPLE STEREOCHEMISTRY IN COPPER(II) HALIDES

ROGER D. WILLETT
Department of Chemistry, Washington State University, Pullman, WA 99164–4630 (U.S.A.)

(Received 21 August 1990)

CONTENTS

A. Introduction 181
B. The charge compensation principle 183
C. Coordination geometry 184
  (i) Distortions in six-coordinate species 184
  (ii) Distortion in four-coordinate species 185
  (iii) Distortions in five-coordinate species 186
D. Bridging modes in extended systems 188
E. Structure descriptions 189
  (i) $(1,4\text{-DMP})_4Cu_5Cl_{14}$ 192
  (ii) The $Me_nEt_{4-n}N$ chloride salts 193
  (iii) $(Me_4P)Cu_2Cl_5$ 196
  (iv) $(C_6H_{18}N_3)_4Cu_5Cl_{22}$ 197
  (v) A_2CuCl_4 salts 197
  (vi) $[Et_2NH_2]_2Cu_4Br_{10}\cdot C_2H_5OH$ 199
  (vii) $A_2Cu_nX_{2n+2}$ oligomers 200
  (viii) $(Et_4N)_8Cu_{14}Cl_{28}O_4$ 201
F. Conclusions 202
References 204

A. INTRODUCTION

The organic ammonium salts of copper(II) halides show a wide variety of stereochemical complexity. Due to the Jahn–Teller effect, high symmetry stereochemistries represent maxima in the potential energy surface for the Cu(II) ion [1]. The position of the minima is dependent upon a wide variety of internal and external forces. This induces an inherent flexibility in the Cu(II) coordination sphere, one feature of which allows for both normal Cu–X bonds and longer, semi-coordinate Cu···X bonds. Observed geometries include four-coordinate species (ranging from square planar to nearly tetrahedral) [2], five-coordinate species (spanning trigonal bipyramidal, square pyramidal, and folded or tetrahedrally distorted 4+1 geometries) [3], and

0010-8545/91/$8.75

six-coordinate species (generally with tetragonally elongated octahedra 4+2 geometries) [4]. The non-stereospecific nature of the rather large, spherical, negatively charged halide ions also plays a fundamental role in determining the actual geometries obtained.

The bridging ability of the halide ions further complicates the crystal chemistry of copper(II) halide salts. The bridge formation can involve either two normal Cu–X bonds (a symmetrical bridge) or one normal Cu–X bond and one longer semi-coordinate Cu···X bond (an asymmetrical bridge). In addition, pairs of Cu(II) ions can be bridged combinations of one, two or three such bridges. The bridges may involve only a finite number of Cu(II) ions, defining oligomeric units which range from 2 to 14 Cu(II) ions, or may form infinitely extended one-, two-, or three-dimensional polymeric species. Thus a bewildering array of solid state structures is possible.

Some semblance of sanity can be extracted from these structures, and a reasonable rationalization made for many of the structures by application of simple electrostatic arguments to which we have applied the term 'charge compensation'. Naively, the observed stereochemistries of Cu(II) halide salts can be visualized as a balance between crystal field stabilization effects and an electrostatic ligand–ligand repulsion effect. The former favor a square planar arrangement for the normal coordinate bonds while the latter help stabilize a tetrahedral-type geometry. The square pyramidal geometry lies between these two extremes while the trigonal bipyramidal geometry appears to be rather unfavorable due to the second-order Jahn–Teller effect [5]. Thus any factors, such as hydrogen bonding, which reduce ligand–ligand repulsions should lead to stabilization of the square-planar, folded 4+1, and 4+2 geometries. One might anticipate these geometries to be predominant more in chloride salts of organic ammonium ions than in the corresponding bromide salts, both because of lesser ligand–ligand repulsions and stronger hydrogen bonding. Involvement of the halide ions in bridge formation will produce similar behavior, with symmetric bridge formation more effective than asymmetric bridge formation at stabilizing the planar geometry. These arguments have been used to explain much of the observed structural chemistry for $ACuCl_3$ salts [6] as well as the crystal chemistry of the antiferrodistortive A_2CuX_4 layer perovskites [4].

These factors proved to be particularly useful in understanding the thermochromic behavior of copper(II) salts [7] where comparisons could be made between the coordination geometries of two phases of the same compound. The delicate balance between these various factors can be even more clearly seen where two (or more) of these geometries occur in the same structure. In this article the structures of copper(II) halide systems *which contain multiple coordination geometries* are discussed in terms of the above-mentioned charge compensation effects.

B. THE CHARGE COMPENSATION PRINCIPLE

In this section we will look at the stereochemistry of copper(II) halides and detail the variations in coordination geometry that arise. Halide ions place no direct constraints upon the copper(II) geometry, as would be the case for polydentate ligands or multi-atom ligands. On the other hand, the chloride and bromide ions are large enough that ligand–ligand repulsion effects are not negligible. This appears to provide access to a larger portion of the potential surface for these complexes and thus gives us a better chance to examine its peculiarities. (Square planar coordination dominates for fluoride salts, while iodide salts are thermodynamically unstable. Thus this review will be limited to the chloride and bromide systems.) The factors which influence the stereochemistry of copper(II) halides can be grouped into five categories.

(i) Jahn–Teller effect. The Jahn–Teller theorem states that, for odd electron systems, species with electronic ground states which are orbitally degenerate will have a tendency to distort along a symmetry coordinate so as to remove that degeneracy. In a sense, this is a negative stereochemical factor, in that it only tells us what geometries should not exist. For the d^9 Cu(II) system, this precludes the octahedral and tetrahedral geometries. Unfortunately, the theorem does not tell us how far, or even in which direction, the molecule will distort. This depends in detail on the strength of the coupling between the electrons and the underlying lattice. Since large distortions are generally observed for Cu(II) species, it must be presumed that this coupling is large.

(ii) Crystal field stabilization. This arises because of the directional character of the metal *d* orbitals, which results in a lifting of their degeneracy upon bond formation with the ligands. In general, for a d^9 system, the greatest stabilization will occur for the geometry which gives the strongest bonding. If this were the only factor which were relevant in determining the stereochemistry, one would expect all Cu(II) complexes to be square planar.

(iii) Ligand–ligand repulsions. The electrostatic repulsions between the halide ions will also play an important role in determining the coordination geometry since it greatly favors tetrahedral geometry.

(iv) Ligand–lattice interactions. In this category are the primarily electrostatic interactions between the halide ions and their environment, including simple electrostatic interactions between the halide ions and the counterions, bonding interactions with neighboring Cu(II) ions, as evidenced by the formation of Cu–X–Cu bridges; hydrogen bonding interactions between the halide ions and either the counterions or lattice solvent molecules. Each of these has the effect of reducing the effective charge on the halide ions, which in turn reduces the ligand–ligand repulsion effects.

(v) Crystal packing effects. This category lumps together all effects not

contained in the previous categories. In particular it recognizes that the shape of the counterions may predispose the lattice to some particular form and the copper(II) halide species may have to adapt its stereochemistry to best be accommodated into that packing arrangement.

The principle of charge compensation, simply stated, is that each halide ion will interact as strongly as possible with sources of positive charges in the lattice. This provides for charge balance within the lattice and, from the stereochemical point of view, greatly reduces ligand–ligand repulsion effects. As these ideas are applied throughout this review, it will be seen that they at least provide a mechanism for correlating and interpreting the observed structures, and hopefully will provide insight into the prediction, design and synthesis of new systems.

C. COORDINATION GEOMETRY

In this section, a brief summary of some of the important features of the various coordination geometries observed in copper(II) halide species will be given. For more details, the reader is referred to more recent discussions for four-coordinate $CuCl_4^{2-}$ anions [2], five-coordinate species [3], and six-coordination in layer perovsites [4], in addition to the original summary of Smith [8].

(i) Distortions in six-coordinate species

Experimentally, it is observed that the predominant distortion of the six-coordinate species leads to a geometry with four short and two long copper–ligand distances (4+2 coordination). The magnitude of the distortion depends upon the details of the shape of the potential surface. Thus, the D_{4h} elongation can range from a very small amount, e.g. distorted octahedron, to the limiting situation where the axial ligands are completely disassociated, yielding a square-planar complex.

The presence of the 4+2 geometry leads to the concept of semi-coordination; that is, based on many structural and spectroscopic properties, the existence of a copper–ligand interaction which is distinctly weaker than the primary copper–ligand interactions. A convenient operational definition for semi-coordination is based on ligand–ligand contacts, rather than on some arbitrary copper–ligand distance. Thus, for a given ligand, if the intracomplex ligand–ligand distances are greater than the sum of the respective van der Waals radii, the ligand is said to be semi-coordinate. This arbitrary, but easily applicable, criteria is useful in the discussion of the coordination geometry of copper(II) species.

In addition to the simple process of elongation of the octahedron to form a centrosymmetric 4+2 species, it is observed that in a non-centrosymmetric environment, the two semi-coordinate distances tend to deviate from their mean value. This is seen in Fig. 1 where, for a series of stacked oligomers, the difference, Δ, between the two semi-coordinate distances are plotted versus the shorter of the two [9]. It is seen that Δ reaches values of up to 0.6 Å, and thus one really observes what should be more properly specified as a 4+1+1 geometry.

(ii) Distortion in four-coordinate species

The distortion of tetrahedral Cu(II) species is generally found to occur as a substantial compression of the tetrahedron along one of its S_4 axes, yielding a complex of D_{2d} symmetry. In the limit, this distortion carries the species over to the square planar complex. The distortion pathway of the isolated $CuCl_4^{2-}$ ion from tetrahedral to square planar is one of the most studied potential surfaces in inorganic chemistry [2]. It is convenient to denote the extent of distortion by θ, the average of the two *trans* Cl–Cu–Cl angles, which varies from 180° in the square planar limit to 109.5° in the tetrahedral limit. More than 60 structures have been determined. As can be seen in Fig. 2, the majority occur with θ between 130 and 140°. A rather substantial gap from 155 to 165° occurs. Thus the experimental data might indicate a double

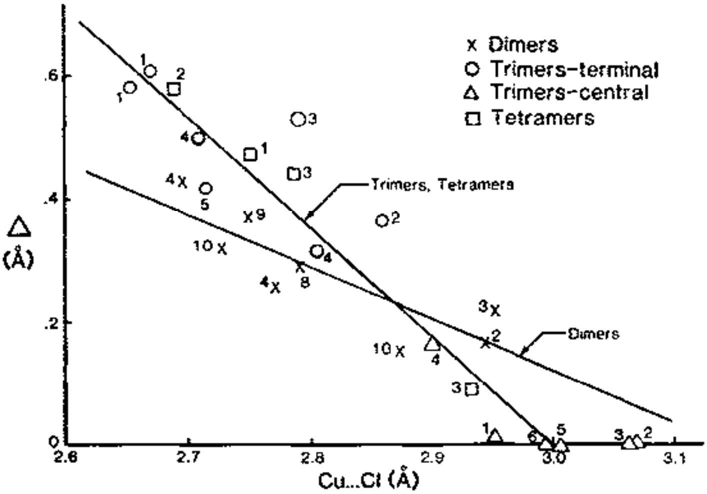

Fig. 1. Plot of the difference, Δ, between the two semi-coordinate Cu···Cl distances versus the shorter Cu···Cl distance for $Cu_nCl_{2n}L_2$ oligomers. The number by each data point corresponds to the place in which the oligomer occurs in its category in Table 1 in ref. 9. (From ref. 9.)

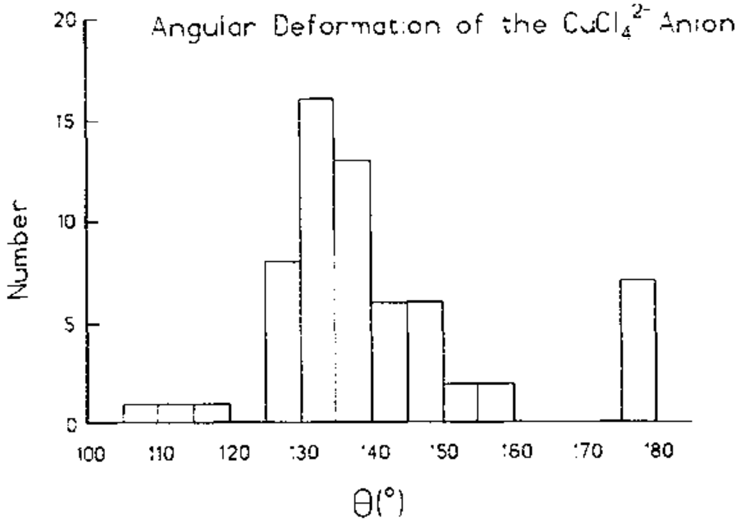

Fig. 2. Distribution of *trans* Cl–Cu–Cl angles, θ, for 62 known $CuCl_4^{2-}$ anions. (From ref. 2.)

minima potential surface, one near $\theta = 135°$ and one near $\theta = 180°$. Values of θ near 109.5° are likely to arise because of the disorder.

This is where the application of the principle of charge compensation first came into usage. It was observed [10] that $CuCl_4^{2-}$ ions with large bulky counterions assumed a geometry near the tetrahedral limit, while those where the counterions had strong hydrogen bonding capabilities were much closer to the square planar limit. Thus, it was argued that the hydrogen bonding effectively removed charge from the halide ions, which reduced the ligand–ligand repulsions. The crystal field effects then dominated and the more planar geometry could be assumed.

(iii) Distortions in five-coordinate species

The geometries of five-coordinate copper complexes are quite varied. The idealized symmetrical end members of square pyramidal and trigonal bipyramidal geometries are observed rather rarely. Instead, a rather ill-defined stereochemistry involving four normal copper–ligand (Cu–L) bonds and one longer, so-called semi-coordinate (Cu–L′) bond is commonly observed (Fig. 3(a)). However, to describe the geometry more completely, it is necessary to specify the L–Cu–L′ angles since a significant number of 4+1 species distort toward tetrahedral geometry for the CuL_4 moiety. In the subset of the 4+1 geometries that excludes the tetrahedral distortion, a large number have an elongated Cu–L′ distance with one *trans* L–Cu–L′ angle of approximately 180°. We will refer to this as a folded geometry.

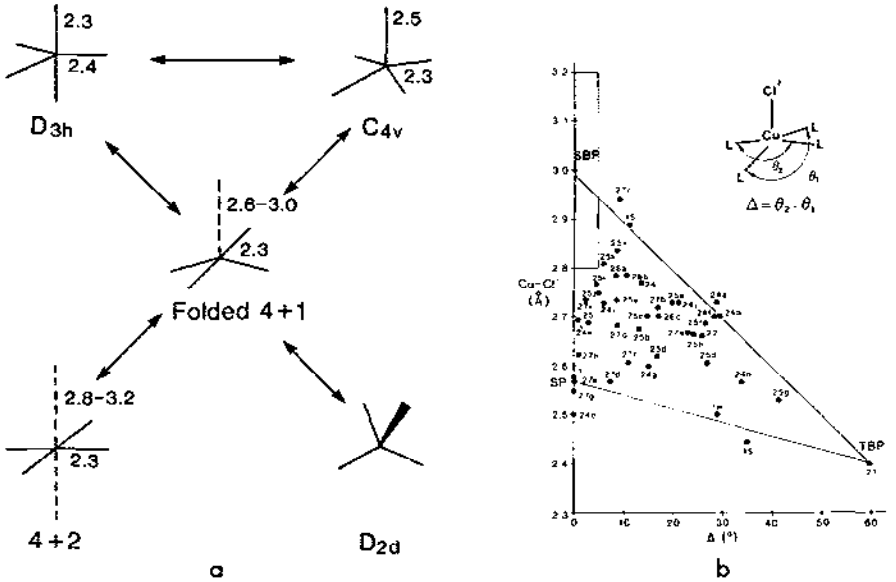

Fig. 3(a). Common limiting coordination geometries for copper(II) halides. (b) Plot of semicoordinate Cu–Cl distances versus the angular distortion, Δ, for five-coordinate copper(II) chloride species. The numbers refer to references in ref. 3.

To characterize the five-coordinate surface, the structural data on a large number of folded copper(II) chloride salts and/or complexes have been tabulated with the requirement that L' and at least two of the L ligands are chloride ions [3]. Figure 3(b) plots the Cu–L' distance versus Δ, the difference between the two *trans* angles. This two-dimensional plot is not unambiguous, since it does not indicate the deviations of the larger of the angles from 180°. However, this is normally in the range 170–180°, except for the square-pyramid limit. The points labeled SP and TBP define the square-pyramidal (in $(C_6H_{18}N_3)CuCl_5{\cdot}H_2O$ [11]) and trigonal-bipyramidal (in the $Cu_4Cl_6OL_4$ clusters [12]) limits. Also indicated by the shaded region is the square-bipyramidal limit, designated by SBP, of the 4+2 coordination geometry. In this geometry, the semicoordinate bonds typically range from 2.8 to 3.2 Å. As can be seen, there is a wide scatter of geometries represented on this diagram. Nevertheless, it is possible to observe a preferred region on this section of the potential surface defined by a Cu–Cl' distance in the range 2.65–2.75 Å and $15° < \Delta < 30°$. This folded 4+1 stereochemistry then must be recognized as the dominant five-coordinate geometry in copper(II) halide chemistry. Conspicuous by their absence, other than in the $Cu_4Cl_6OL_4$ clusters, are geometries approaching the TBP limit. Thus the experimental evidence demonstrates that this geometry is not favored, as argued theoretically by Reinen and Atanasov [5]. There are a number of compounds in which the geometries approach the SP limit, which indicates that the potential surface has a rather low energy in this limit. An interesting question, unresolved by the data at this point, is whether or not a potential barrier exists between the SP and folded 4+1 geometries. Finally, it is noted that only two compounds exist along the direct SP–TBP pathway.

D. BRIDGING MODES IN EXTENDED SYSTEMS

In the discussion of coordination geometry, two types of coordination were recognized: normal coordinate bonds and longer, semi-coordinate bonds. When a halide ion bridges between two copper(II) ions, it can do so via two normal bonds (a symmetric bridge) or via one normal and one semi-coordinate bond (an asymmetric bridge). Bridges involving two semi-coordinate bonds are generally not observed.

Two copper(II) ions may be bridged by one, two or three halide ions. The most common bridging modes involve (a) two symmetric bridges, as in anhydrous $CuCl_2$ [13] and $CuBr_2$ [14]; (b) two asymmetric bridges, as in $CuCl_2{\cdot}2H_2O$ [15]; or (c) three bridges with one symmetric type and two asymmetric types, as in $CsCuCl_3$ [16]. Less frequently found is one asymmetric bridge, as in $CuCl_2{\cdot}2DMSO$ [17]. Only one or two examples are known of single symmetric bridges ($CsCuBr_3$ [18]) and of mixed symmetric/asymmetric bibridges (in $(Et_4N)_4Cu_4Cl_{12}$ [19]).

The bridging of the halide ions is one of the main mechanisms of charge compensation available to the lattice to reduce the effective charge on the halide ion. This has two effects: it helps stabilize the square planar coordination geometry for the normal coordinate bonds and it lengthens the normal coordinate bonds substantially. The symmetric bridges will be more effective in this than the asymmetric bridges. In addition, this charge compensation mechanism works in a complementary fashion to the hydrogen bonding and other ligand–lattice mechanisms: halogens which are extensively involved in bridging will not form hydrogen bonds, and vice versa.

This role of bridging stabilizing the planar geometry for the principle coordination is clearly seen in the structural properties of salts containing $Cu_2Cl_6^{2-}$ anions. As previously discussed, the isolated $CuCl_4^{2-}$ anion prefers a compressed tetrahedral geometry with a *trans* Cl–Cu–Cl angle of 135°. In isolated $Cu_2Cl_6^{2-}$ oligomers, which contain a symmetrical bibridged arrangement, this angle is opened up to 145° [20]. When both semi-coordination sites are occupied, either by chloride ions from adjacent dimers or by other ligands, the dimer unit is essentially planar [21]. As the coordination geometry distorts from a 4+2 geometry through the 4+1+1 arrangement to eventually a 4+1 geometry, the coordination geometry is progressively folded until one of the *trans* Cl–Cu–Cl angles approaches 145° while the other remains near 180° [22]. These changes are illustrated in Fig. 4.

The stability induced by the formation of these bridging arrangements is evidenced by the large number of oligomeric and polymeric structures which have been observed. Quasi-planar symmetric bibridged oligomers with stoichiometry $Cu_nX_{2n+2}^{2-}$ have been found for values of $n = 1-7$ [23,24]. Structural characteristics of the oligomers have been summarized [9,20], as well as details of their stacking arrangements for $n \geq 2$ [23]. The charge compensation ideas have been applied to a series of bi- and tribridged $ACuCl_3$ structures [25]. Asymmetric bridged species exist in a wide variety of dimeric species [26] and infinite chains [27].

E. STRUCTURE DESCRIPTIONS

There have been numerous copper(II) halide complexes reported in which two or more distinctly different coordination geometries appear in the crystal structure. These are tabulated in Table 1. Thus qualitative charge compensation ideas may be used to interpret the main features of the structural results, while at the same time pointing out some of their limitations. In particular, because of the flatness of the potential surfaces, the ever-ubiquitous packing forces will certainly dominate in some cases.

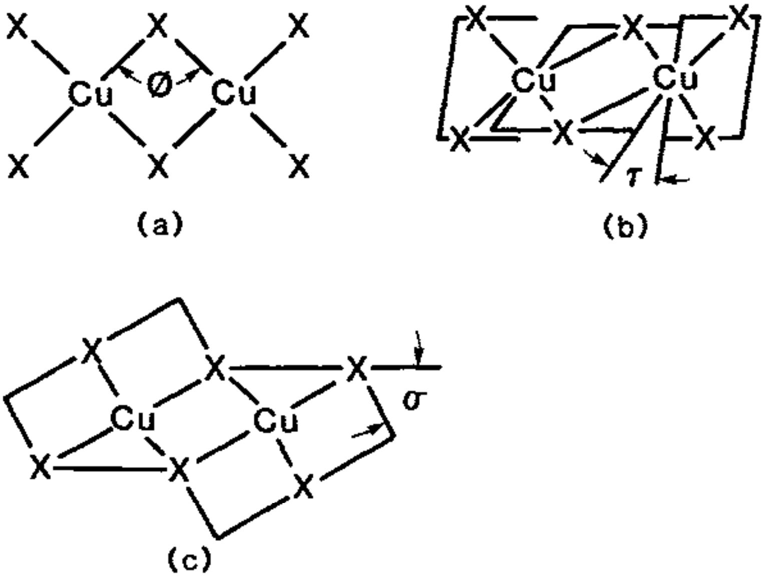

Fig. 4. Illustration of the geometry of $Cu_2Cl_6^{2-}$ dimeric species (a) planar, (b) twisted, (c) folded.

TABLE 1

Summary of stereochemistries in copper(II) halide salts with multiple stereochemistries

Compound	Stereochemistry[a]	Bridging halides[b]	Hydrogen bonds[c]	Ref.
(1,4,-dimethylpyridinium)Cu_5Cl_{14}	4+2 (2.868 Å)	4,2	0	28
	5 (2.456 Å, sp)	5	0	
	4 (133.2°)	2	0	
$(Et_4N)_4Cu_4Cl_{12}$	4+1 (2.662 Å, tet)	3,1	0	19
	4 (141.4°)	2	0	
$(Me_2Et_2N)_4Cu_4Cl_{12}$	4+1 (2.628 Å, tet)	3,1	0	32
	4 (136.7°)	2	0	
$(MeEt_3N)_3Cu_3Cl_9$	5 (2.468 Å, tbp)	4	0	32
	4 (146.6°)	2	0	
$(EtMe_3N)_4Cu_5Cl_{14}$	4+2 (2.907 Å)	4,2	0	28
	4+1+1 (2.694, 3.273 Å)	4,2	0	
	4+1 (2.606 Å, sp)	4,1	0	
$(Me_4P)Cu_2Cl_5$	5 (2.573 Å, sp)	5	0	23
	4+1+1 (2.681, 3.371 Å)	4,2	0	
[*N*-(2-ammonioethyl)-piperazinium]$_4Cu_5Cl_{22}$	4+2 (2.971 Å)	0,2	4	35
	4+1 (2.719 Å)	0,1	4	
	4 (125.6°)	0	0	
	4 (141.8°)	0	0	
$[(C_2H_5)_2NH_2]_2CuCl_4$ (Room T)	4 (145°)	0		36
	4 (159°)	0		
	4 (178°)	0		
(*N*-benzylpiperazinium)$_2CuCl_4$	4 (137°)	0	3	37
	4 (151°)	0	3	
$(CuL_3)_2Cu_2Cl_6$ ($L=(\phi_2PO)_2CH_2$)	4 (124.8°)	2	0	38
	4 (143.2°)	2	0	
$[(CH_3)_2CHNH_3]_2CuCl_4$ (Room T)	4+2 (3.070, 3.103 Å)	2,2	8,8	39
	4+1 (3.326, 3.123 Å)	1,1	5,6	

$[(C_2H_5)_2NH_2]_2Cu_3Br_8CuBr_2C_2H_5OH$	4+2 (3.241) Å	4,2	2	40
	4+2 (3.236 Å)	2,2	0	
	4 (116.9°)	4	0	
$[(C_2H_5)NH_2]_8Cu_{14}Cl_{28}O_4$	5 (tbp)	4	0	42
	4+1 (2.709–2.828 Å, sp)	2,2	0	
	4+1 (3.100 Å, tet)	3,1	0	

---

[a] Axial Cu–Cl bond lengths for 4+2, 4+1, and 5 coordinate species and average *trans* Cl–Cu–Cl bond angles for 4 coordinate species are listed. The dominate coordination geometries of 4+1 or 5 coordinate compounds (square pyramidal (sp), trigonal pyramidal (tbp), or tetrahedral (tet)) are also listed.

[b] Listed as *m*, *n* pairs, where *m* is the number of normally coordinated halides involved in bridging and *n* is the number of semicoordinate halides involved in bridging.

[c] Number of N–X distances less than 3.3 Å (X=Cl) or 3.4 Å (X=Br).

(i) (1,4-DMP)$_4$Cu$_5$Cl$_{14}$

This crystal structure, where 1,4-DMP = 1,4-dimethylpyridinium, gives one of the most dramatic demonstrations of the coexistence of multiple copper(II) halide stereochemistries in a single compound [28]. It consists of infinite $(Cu_5Cl_{14}^{4-})_n$ 'knobby' chains. Within the chains (Fig. 5), three distinct coordination sites exist: Cu(1), at a site of $\bar{1}$ symmetry, with a 4+2 coordination geometry; Cu(2) with a distorted square pyramidal geometry; and Cu(3) with a distorted tetrahedral coordination geometry. The chain itself consists of repeating Cu(1)–Cu(2)–Cu(2) sequences, each adjacent pair of copper ions linked by two symmetrical Cu–Cl–Cu bridges. The configuration of the Cu(2)–Cu(2) linkage is very close to that observed in a series of stacked bifolded $Cu_2Cl_6^{2-}$ dimers [22], while the Cu(2)–Cu(1)–Cu(2) grouping has a conformation closer to that observed in stacked, planar $Cu_3Cl_8^{2-}$ trimers [29]. The tetrahedra associated with the Cu(3) ions form the 'knobs' on the chains, bridging between neighboring Cu(1) and Cu(2) ions in the trimeric unit. These linkages between the tetrahedral copper ion and the copper ions in the chain involve a symmetrical bridge to Cu(2) and an asymmetrical bridge to Cu(1).

Associated with the $Cu_5Cl_{14}^{4-}$ grouping described above are two pairs of crystallographically inequivalent 1,4-DMP cations. Both cations form long N–Cl interactions with the non-bridging chloride ions of the tetrahedral

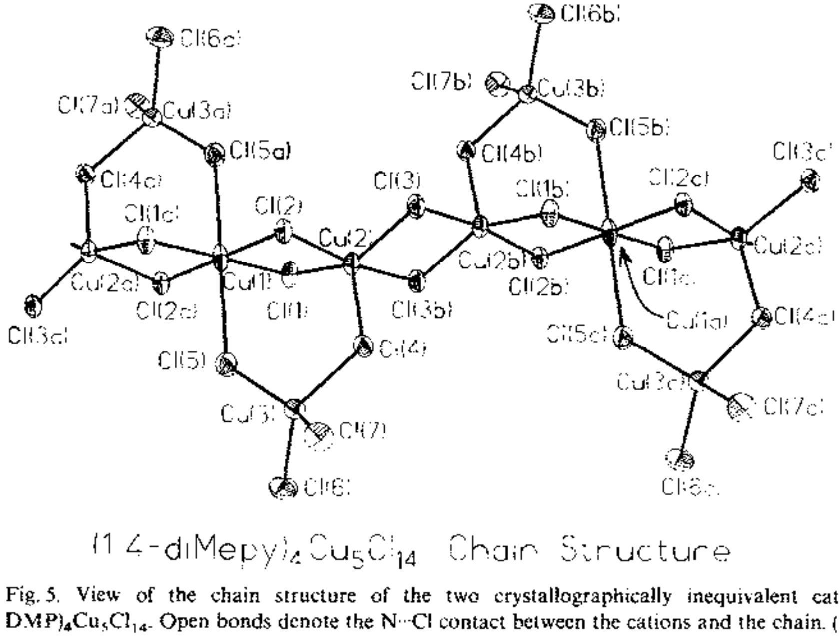

Fig. 5. View of the chain structure of the two crystallographically inequivalent cations in (1,4-DMP)$_4$Cu$_5$Cl$_{14}$. Open bonds denote the N···Cl contact between the cations and the chain. (From ref. 28.)

copper species with contact distances (3.47 Å) which are comparable in length with those observed in other quaternary pyridinium halometallates [30].

The application of the charge compensation ideas to this structure is quite straightforward. The chloride ions involved in the symmetric bridges find electrostatic repulsion reduced to the point where the crystal field stabilization energy dominates. Thus Cu(1) assumes a planar configuration, allowing for the formation of two semi-coordinate bonds, while Cu(2) takes on a square pyramidal conformation. Of the chloride ions bonded to Cu(3), two are involved in bridge formation (one symmetric, one asymmetric). The other two are involved in no direct charge compensation mechanisms, their only contacts are with the 1,4-DMP cations. Thus the coordination geometry is dominated by the electrostatic repulsions between the halide ions, and only a small distortion from a tetrahedral geometry is observed.

(ii) The $Me_nEt_{4-n}N$ chloride salts

The structural chemistry of this series of salts, for $n = 0$–4, provide an interesting demonstration of the sensitivity of the Cu(II) halide stereochemistry upon small changes in the environment of the copper halide species, and why prediction of structure based on the simple charge compensation effects is tenuous at best. The structures of the two end members ($n = 0$, 4) have been known for some time. The $(Me_4N)CuCl_3$ salt contains tribridged $(CuCl_3^-)_n$ chains in which each Cu(II) ion has a 4+2 coordination. In each chain, there are five crystallographically inequivalent Cu(II) ions. The compound undergoes intriguing cooperative dynamic Jahn–Teller phase transitions [31]. The structure of the Et_4NCuCl_3 salt was reported several years ago [19], while the remainder have been examined in the hope that additional tribridged structures could be prepared. The $n = 0$–3 salts all proved to contain copper(II) oligomers or polymers possessing two or more stereochemistries.

The tetrameric salt $(Et_4N)_4Cu_4Cl_{12}$ [19] (Fig. 6) superficially contains several of the features of the 1,4-DMP salt described above. The conformation of the central Cu(1)–Cu(1) linkage in the tetramer is similar to that of the Cu(2)–Cu(2) linkage in the chain system. However, the axial bond length is substantially longer in the tetramer, and a small tetrahedral distortion is superimposed on the basal plane of the Cu(2) complex in the chain. The terminal Cu(2) ions of the tetramer are tetrahedrally coordinated, by analogy to the Cu(3) coordination sphere in the knobby chain system. It is also linked to the remainder of the system by one symmetrical and one asymmetrical bridge. Here, however, both bridges are to a single copper ion.

The application of charge compensation arguments to the tetramer is straightforward. For Cu(2), four of the five chloride ions bonded to it are

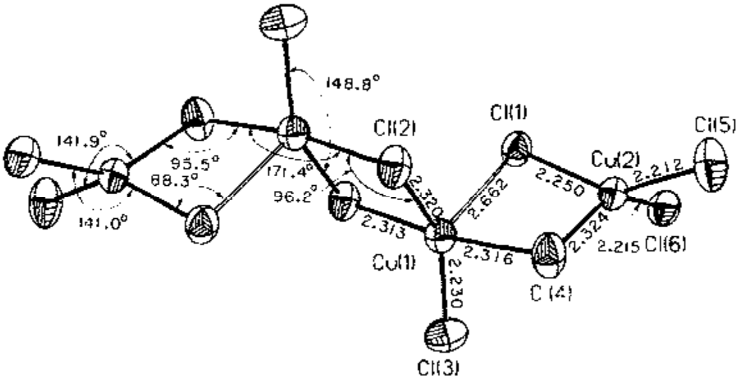

Fig. 6. View of the $Cu_4Cl_{12}^{4-}$ tetrameric species in the $[(C_2H_5)_4N]_4Cu_4C_{12}$ structure. (From ref. 19.)

involved in bridges (three symmetrical, one asymmetrical) to other copper ions. Thus, the crystal field factors dominate, and a distorted 4+1 geometry is assumed. For Cu(2), only one chloride participates in a symmetric bridge, and one other in an asymmetric bridge. With no possibility for the other two chloride ions to participate in hydrogen bonding or other effective charge compensation mechanisms, the distorted tetrahedral geometry follows. The cations are located near the non-bridging halide ions, so as to maximize electrostatic interactions.

The structure of the anionic species in $(Me_2Et_2N)_4Cu_4Cl_{12}$ is identical to that in the Et_4N^+ salt [19]. In contrast, the $MeEt_3N^+$ salt forms a trimeric species of stoichiometry $(MeEt_3N)_3Cu_3Cl_9$, as seen in Fig. 7 [32]. This has many of the same features of the tetramers, but the central Cu(II) ion now has very nearly a trigonal bipyramid geometry, with the major deformation

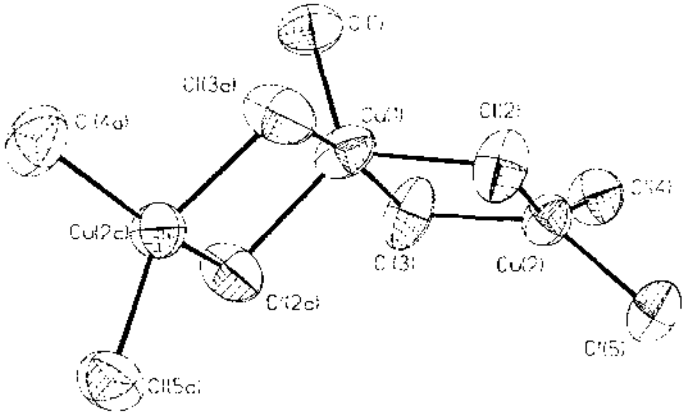

Fig. 7. Illustration of the $Cu_3Cl_9^{3-}$ trimeric species in $(MeEt_3N)_3Cu_3Cl_9$.

a bending of the axial Cl–Cu–Cl angle from the ideal of 180 to 162°. The charge compensation arguments are essentially the same as those for the tetrameric species. In particular, it is found that one set of $MeEt_3N^+$ cations is located near the non-bridging Cl atom on the central Cu(II) ion, while the other two sets of $MeEt_3N^+$ are located near the non-bridging Cl atoms on the terminal Cu(II) ion.

The structure $(Me_3EtN)_4Cu_5Cl_{14}$ consists of $(Cu_5Cl_{14}^{4-})_n$ linear chains, as seen in Fig. 8, with the chains isolated from one another by the bulky Me_3EtN^+ cations. The pentameric repeat unit of the inorganic chain has inversion symmetry and contains copper ions in three distinct coordination geometries. The central copper ion of the pentamer sits on a center of inversion and exhibits a distorted octahedral 4+2 coordination geometry. The two other crystallographically independent copper(II) ions of the pentamer exhibit distorted square pyramidal geometries, however the amount of distortion is very different in the two cases. The coordination geometry about Cu(2) is close to square pyramidal (Cu(2) also forms a long, semicoordinate bond with Cl(3), 3.273 Å, so the actual geometry is 4+1+1′). The geometry about Cu(3) is strongly distorted toward trigonal bipyramidal. The Cu–Cl bond lengths are similar to those Cu(2); however, one of the basal chlorides is distorted out of the plane formed by the other three basal ligands, forming an angle of 120.6(1)° with the axial chloride.

In this case, the attempt to prepare a tribridged chain analogous to that in Me_4NCuCl_3 was nearly successful. Examination of Fig. 8 shows that four of every five Cu···Cu bridges are of the tribridged variety. Unfortunately, two chloride bridges between square pyramidal copper(II) ions link adjacent pentameric units in the chain, as in the 1,4-DMP salt. Since all chloride ions are involved in bridges between copper ions, one can understand why, based on charge compensation arguments, the tetrahedral geometry is absent from the chain. The inversion center about Cu(1) favors the observed 4+2 geometry while the presence of the distant axial chloride in the 4+1+1′ geometry of Cu(2) prevents distortion of any of the basal chlorides out of the plane preserving the square pyramidal geometry. Cu(3), on the other hand, exhibits a severe distortion of the trigonal bipyramidal geometry and its coordination

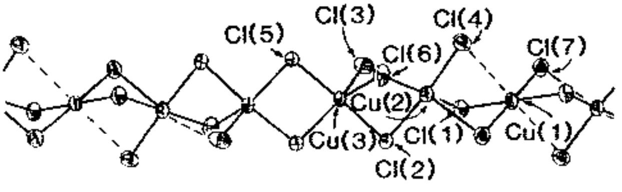

Fig. 8. View of the chain structure in $(Me_3EtN)_4Cu_5Cl_{14}$. Broken lines indicate semicoordinate Cu···Cl bonds. (From ref. 28.)

sphere is best described as intermediate between square pyramidal and trigonal bipyramidal. The cause of these differences in geometry of the copper(II) ions is certainly more complex than can be treated by the crude 'charge compensation' ideas. In the absence of a more complete theory, we must attribute these differences to 'packing forces'.

(iii) $(Me_4P)Cu_2Cl_5$

Along this same vein, Maaskant and coworkers attempted to prepare an analog of $(Me_4N)CuCl_3$ by utilizing the corresponding phosphonium cation in place of the conventional ammonium cation. They isolated, instead of the desired trichloride, a salt of stoichiometry $(Me_4P)Cu_2Cl_5$, which contains a complicated two-dimensional network (Fig. 9) [33]. The coordination geometry of one Cu(II) ion is very near to square pyramidal (Cu–Cl (axial) = 2.573 Å, with *trans* Cl(eq)–Cu–Cl(eq) angles of 160.1 and 166.9°), while that of the second ion is better described as a 4 + 1 + 1 coordinate species (Cu···Cl = 2.681 and 3.37 Å) with a small tetrahedral distortion superimposed on the basal plane. The Me_4N^+ salt of this stoichiometry contains stacks of quasi-planar symmetrically bibridged $Cu_4Cl_{10}^{2-}$ anions [34].

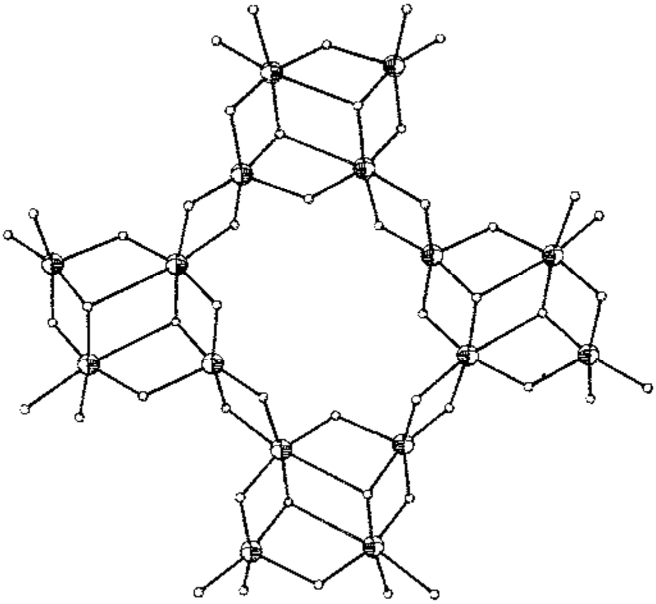

Fig. 9. A portion of the two-dimensional network in $(Me_4P)Cu_2Cl_5$. (After ref. 33.)

(iv) $(C_6H_{18}N_3)_4Cu_5Cl_{22}$

One of the more interesting salts is the *N*-(2-aminoethyl)piperazinium salt of stoichiometry $A_4Cu_5Cl_{22}$ [35]. The structure consists of $Cu_3Cl_{14}^{8-}$ trimers illustrated in Fig. 10, and two crystallographically independent $CuCl_4^{2-}$ anions. The trimer is composed of a planar $CuCl_4^{2-}$ ion semicoordinated by the apical chloride ions of two square pyramidal $CuCl_5^{3-}$ ions. The bridging arrangement is responsible for the elongation of the apical Cu–Cl bond in the square pyramid to 2.719 Å. The square pyramidal coordination is stabilized by extensive hydrogen bonding to the basal chloride ions. The asymmetric bridging of the apical chloride ion provides an additional charge transfer mechanism, which is a major stabilizing factor for the square planar geometry of the central ion. In addition, short hydrogen bonding contacts are made to all four of the chloride ions in the central planar $CuCl_4^{2-}$ unit. In contrast, the two isolated $CuCl_4^{2-}$ anions both have distorted tetrahedral geometries, although the extent of the distortion is significantly different, with *trans* Cl–Cu–Cl angles of 125.6° for Cu(2) and 141.8° for Cu(3). The hydrogen bonding to the halide ions in both anions is relatively long (~3.5 Å) and thus, with no bridge formation and weak hydrogen bonding, the distorted tetrahedral geometry is in accord with the charge compensation ideas.

(v) A_2CuCl_4 salts

The existence of isolated $CuCl_4^{2-}$ ions with different distortions of the tetrahedral geometry is observed in several other salts. The compound $[(C_2H_5)_2NH_2]_2CuCl_4$ contains three crystallographically independent anions, with average *trans* angles of approximately 145, 159 and 178° [36]. Since full structural details were not published, analysis of the differences in the geometries of the sites in terms of the hydrogen bonding scheme has not been made. The green A_2CuCl_4 salt of the *N*-benzylpiperazinium cation

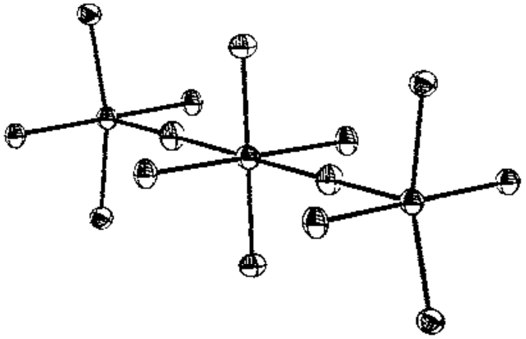

Fig. 10. View of the $Cu_3Cl_{14}^{8-}$ anion in the $(N(2amet)pipz\text{-}H_3)_4Cu_5Cl_{22}$ structure. (After ref. 35.)

contains four inequivalent sites for the $CuCl_4^{2-}$ anions; two with *trans* Cl–Cu–Cl angles of approximately 137° and the other two with *trans* angles near 151°. The authors rationalized these differences in terms of the greater involvement in hydrogen bonding for the latter two anions [37].

A similar variation in the *trans* angles may be found for the asymmetric $Cu_2Cl_6^{2-}$ dimer in a $(CuL_3)_2Cu_2Cl_6$ salt, where L is a diphosphine dioxide ligand [38]. For one copper ion of the dimer, the *trans* angles average 124.8°, while for the second ion the average is 143.2°. Since no hydrogen bonding or bridge formation occurs (except within the dimeric unit) the difference must be attributed to steric packing effects.

The structure of $[(CH_3)_2CHNH_3]_2CuCl_4$ contains two independent ribbons of bridged $CuCl_4^{2-}$ anions [39], as shown in Fig. 11(a). Each ribbon contains two crystallographically independent Cu(II) sites, one with a centrosymmetric 4+2 geometry and one with a tetrahedrally distorted 4+1 coordination geometry. These ribbons may be visualized as slices out of the antiferrodistortive layer perovskite A_2CuCl_4 structure, as illustrated in Fig. 11(b) [4]. As in the layer perovskite structure, the 4+2 geometry is stabilized by the formation of asymmetric bridges by two of the basal chloride ions, as well as by extensive hydrogen bonding by the NH_3^+ moieties of the

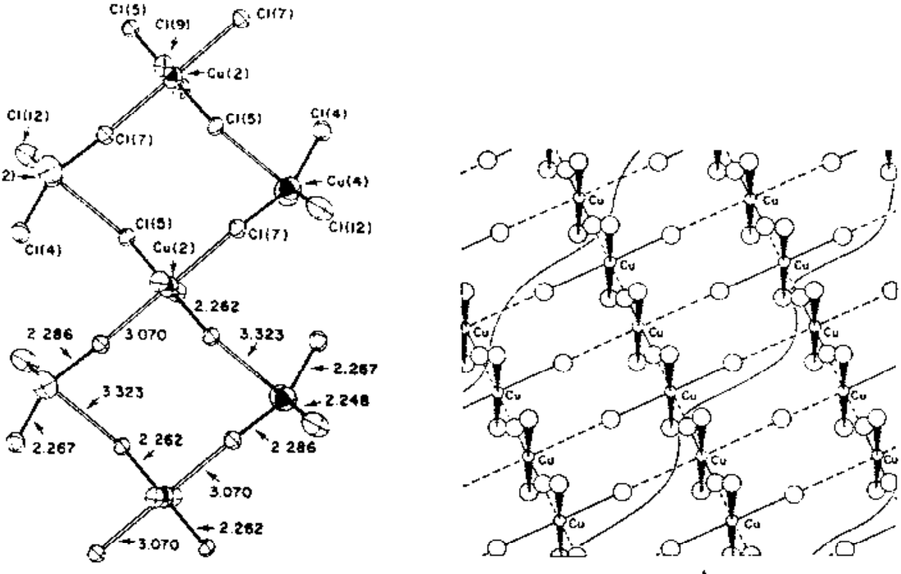

Fig. 11(a). View of a ribbon in the structure of the $[(CH_3)_2CHNH_3]_2CuCl_4$ low-temperature (green) phase. (From ref. 39.) (b) The infinite two-dimensional sheets in the high-temperature (yellow) phase of the $(RHN_3)_2CuCl_4$ salts. The broken lines indicate Cu–Cl distances in excess of 2.8 Å. The curved lines represent possible fracture points for the change to the ribbon structure of the $[(CH_3)_2CHNH_3]_2CuCl_4$ low-temperature (green) phase.

cations, particularly to the non-bridging chloride ions. For the $CuCl_4^{2-}$ anions on the edge of the ribbons, only one of the chloride ions is involved in bridge formation, and the anions distort to a small, but significant, extent toward a tetrahedral geometry. The average *trans* Cl–Cu–Cl angles are 152 and 159°, respectively, in the two independent chains.

(vi) $[Et_2NH_2]_2Cu_4Br_{10}\cdot C_2H_5OH$

The compound $[(C_2H_5)_2NH_2]_2Cu_4Br_{10}\cdot C_2H_5OH$ [40] consists of stacks of planar, bibridged Cu_3Br_8 [40] trimers and neutral bibridged $(CuBr_2)_n$ chains. These are illustrated in Fig. 12. Within the trimers, the copper ions assume a square planar coordination; the stacking causes the presence of longer, semi-coordinate Cu···Br bonds to yield a 4+2 coordination geometry. In contrast, the copper ions in the bibridged chains assume a geometry very close to tetrahedral. The bridging bromide ions in both the trimers and chains are involved in symmetrical bridge formation. The hydrogen bonding of the cations and the EtOH group is primarily to the terminal halide ion of the trimers. These two factors provide adequate charge compensation for all halide ions. Thus it would seem reasonable that the copper ions should have the same geometry in both situations. This difference must be attributed to

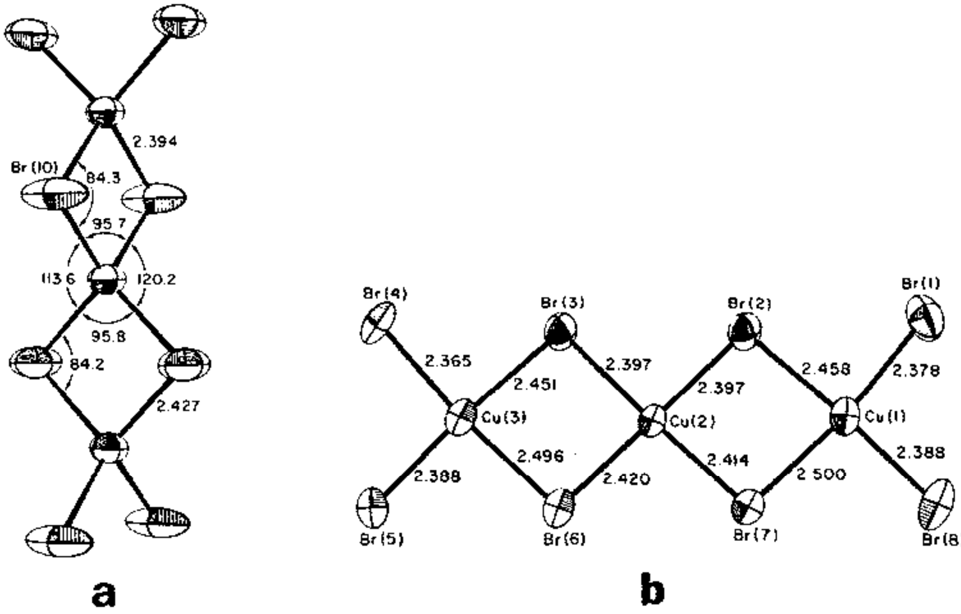

Fig. 12(a). The neutral $CuBr_2$ chain in $(Et_2NH_2)_2(Cu_3Br_8)\cdot CuBr_2\cdot C_2H_5OH$. (From ref. 40.) (b) View of the $Cu_3Br_8^{2-}$ anion in the same structure.

packing forces which prohibit the neutral $(CuBr_2)_n$ chains from assuming the stacked planar arrangement found in $CuBr_2$.

(vii) $A_2Cu_nX_{2n+2}$ oligomers

As indicated previously, a large number of quasi-planar bibridged Cu_nX_{2n+2} oligomers exist which assume a surprising variety of stacking patterns through the formation of semi-coordinate bonds [23,24]. Representative patterns are shown diagrammatically for a series of $n = 4$ salts in I–IV. In I, all of the Cu(II) ions attain a 4+2 coordination (in $(4MAP)_2Cu_4Cl_{10}$ [41]), while in II and III, both 4+1 and 4+2 coordination are observed (in $(Me_3NH)_2Cu_4X_{10}$, X = Cl and Br, respectively [23,34]) and only 4+1 coordination found in IV (in $(1\text{-}MepyH)_2Cu_4Cl_{10}$ [24]). The existence of two coordination geometries on the type II stacks can be seen in Fig. 13, for the


I

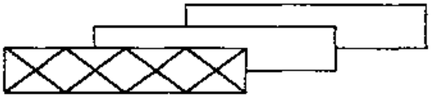
II

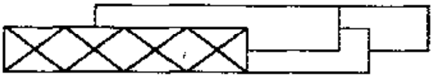
III

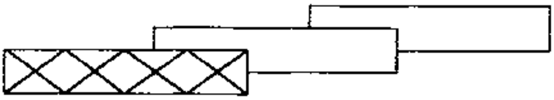
IV

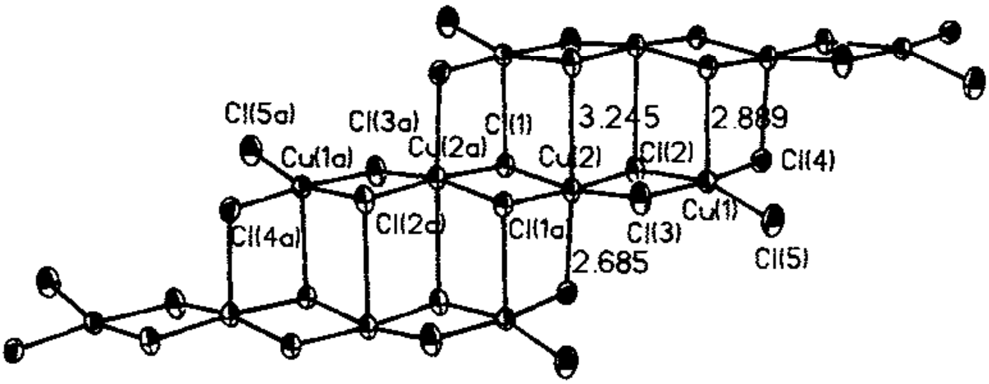

Fig. 13. Illustration of the stacking of $Cu_4Cl_{10}^{2-}$ oligomers in $(Me_4N)_2Cu_4Cl_{10}$. (From ref. 41.)

stacks of tetramers in $(Me_4N)_2Cu_4Cl_{10}$ [41]. Again, the delicacy of the balance of forces defining the structural characteristics is evident, where for the $(Me_4N)_2Cu_4X_{10}$ salts, a type II stack is attained for X = Cl [34], while the Br salt assumes a type III stack [23].

(viii) $(Et_4N)_8Cu_{14}Cl_{28}O_4$

As a final example of a copper(II) chloride salt containing Cu(II) ions with several different coordination geometries, the recently determined structure of $[(C_2H_5)_4N]_8Cu_{14}Cl_{28}O_4$ will be cited [42]. This structure contains copper ions on trigonal bipyramidal, folded 4+1, and tetrahedrally distorted 4+1 geometries. The structure is based on the $Cu_4Cl_6OL_4$ structures (**I** in Fig. 14) found for numerous salts. In this basic (no pun intended) structure, a geometry near trigonal bipyramidal is forced on the copper ion, with an L ligand and an oxygen atom occupying the axial positions *trans* relative to the $CuCl_3$ basal plane. The structure of the $(C_2H_5)_4N^+$ salt can be visualized as built up from the parent $Cu_4Cl_6OL_4$ structure in the following fashion: two Cu_4Cl_6O cores are fused across a common $CuCl_3$ basal plane, as in **II** of Fig. 14; then two such units are then linked as illustrated in **III** of Fig. 14. The distortions which occur in the final structure are illustrated in Figs. 15(a) and (b), where the longer semi-coordinate bonds are shown as open bonds. The views of the two halves of the type **II** unit shown in Fig. 15 are oriented such that the shared $CuCl_3$ basal unit (Cu(4), Cl(1), Cl(2), and Cl(3)) is at the back side of the illustrations.

Because of this condensation of the $Cu_4Cl_6OL_4$ tetranuclear species, the seven independent Cu(II) ions are distributed such that three have trigonal bipyramidal, three have folded 4+1, and one has tetrahedrally distorted 4+1 coordination. The major stereochemical distortions take place because of the interactions across the $CuCl_3$ plane of fusion. As seen in the top portion of Fig. 15, the copper atoms in the Cu_3Cl_6O cap are bowed away from the basal plane, so that the resultant copper–chlorine linkages are elongated. Thus the coordination geometry for those three copper ions is distorted from trigonal bipyramidal to a folded 4+1 geometry with semi-coordinate bond lengths ranging from 2.709 to 2.828 Å. The effect of these distortions is to remove excess charge compensation from the chlorides in the basal plane, so that they are involved in two symmetric and one asymmetric bridges rather than the three symmetric bridges. The tetrahedrally distorted 4+1 coordination occurs because of the linkage of the two type **II** dimeric units. As seen in the lower half of Fig. 15, the involvement of Cl(6) (and the symmetrically equivalent Cl(6a) atom) in this linkage forces a tetrahedral distortion on Cu(3) with the elongation of the Cu(3)–Cl(6a) bond. Again, this removes

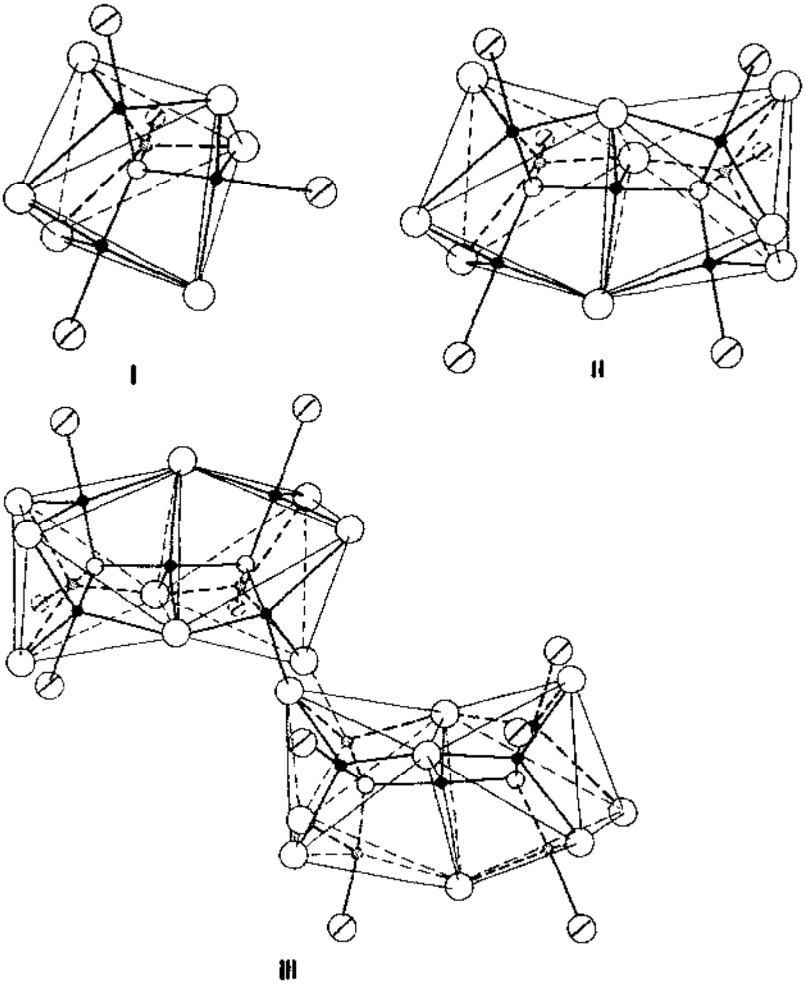

Fig. 14. Illustrations of a $Cu_4Cl_6OL_4$ unit (**I**), of two Cu_4Cl_6O cores fused across a common $CuCl_3$ plane (**II**), and of two of the units in **II** linked to form the basic structure of $[(C_2H_5)_4N]_8Cu_{14}Cl_{28}O_4$. (From ref. 42.)

excessive charge compensation from Cl(6), which would otherwise be involved in three symmetric bridges.

F. CONCLUSIONS

The structures surveyed are examples of an unusual class of metal halide compounds in which the metal ions are found with multiple coordination numbers and/or geometries. Remarkably, the different coordination geometries in many instances occur not about isolated metal ions but in oligomeric

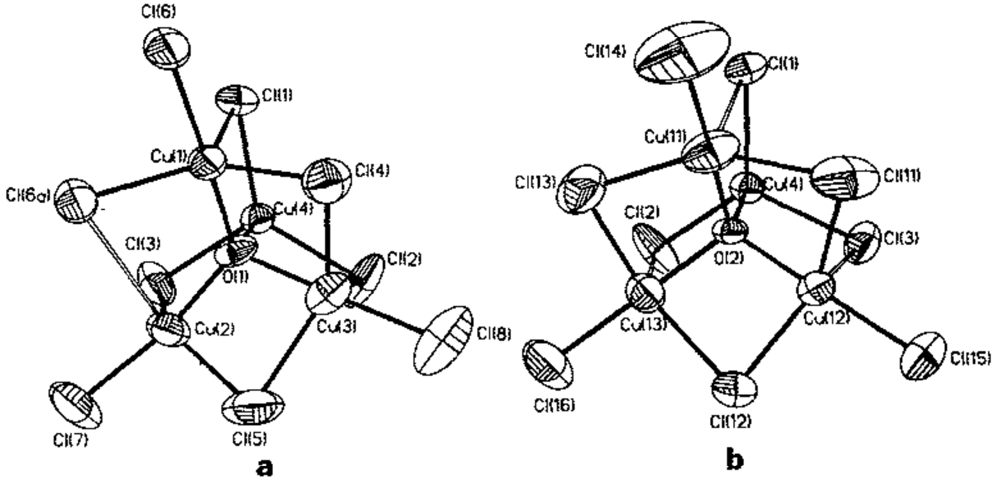

Fig. 15. Illustration of the two halves (a and b) of the type II unit found in the $(Et_4N)_8Cu_{14}Cl_{28}O_4$ structure. (From ref. 42.)

or polymeric structures, illustrating the ease with which the copper(II) ion can assume not only different coordination geometries, but different coordination numbers. The appearance of more than one coordination geometry can frequently be rationalized by an appeal to charge compensation effects.

Such an approach has also been very successful in the past in, for instance, explaining a series of structurally related $ACuCl_3$ uniform chains [24]. If A is a non-hydrogen bonding cation, such as an alkali metal or tetramethylammonium ion, a tetragonally distorted octahedral structure is stabilized by involving all chloride ions in bridging, resulting in the tribridged chain of face sharing octahedra. If the A cation is capable of hydrogen bonding, then the hydrogen bonding provides a competing mechanism for charge removal from the chloride resulting in a chain of symmetrically bibridged square pyramids. Variation in the strength of hydrogen bonding results in a chain with a geometry intermediate between the two extremes. Thus the idea of charge compensation can be very powerful in explaining the variation in geometry of a series of closely related structures.

We must mention the failed attempts to synthesise analogs of the $Me_4N\text{-}CuCl_3$ to point out the limitations of the charge compensation ideas as a predictive tool. By choosing a quaternary ammonium or pyridinium cation for the A ion it was felt that formation of the bibridged structure would be avoided. As should be apparent from the structures described, our initial goal was frustrated. This is no way invalidates the idea of charge compensation, but it underscores the fact that it is only one of several factors which determine the structure. Long-range ionic forces, van der Waals repulsion, and other effects of the crystal 'packing' will play a strong role in determining the geometry of the fluxional Cu(II) coordination sphere as well as long-range geometrical arrangements of the structure. The cation in $(MeEt_3N)_4Cu_5Cl_{14}$, for example, differs from the tetramethylammonium cation by only a single methylene group, yet there is a significant difference between the structures of the inorganic chains in $(MeEt_3N)_4Cu_5Cl_{14}$ and Me_4NCuCl_3. Neither cation can form hydrogen bonds, so the difference in geometry and stoichiometry of the two compounds must be attributed to differences in the ill-defined 'packing forces'.

REFERENCES

1 D. Reinen, Comment Inorg. Chem., 2 (1983) 227.
2 R.D. Willett, K. Halvorson and C. Patterson, Acta Crystallogr., in press.
3 J. Blanchette and R.D. Willett, Inorg. Chem., 27 (1988) 843.
4 R.D. Willett, H. Place and M. Middelton, J. Am. Chem. Soc., 11 (1988) 8639.
5 D. Reinen and M. Atanasov, Chem. Phys., 136 (1989) 27.
6 R.D. Willett and U. Geiser, Croat. Chem. Acta, 57 (1984) 737.
7 D.R. Bloomquist and R.D. Willett, Coord. Chem. Rev., 47 (1982) 125.
8 D.W. Smith, Coord. Chem. Rev., 21 (1976) 93.
9 R.D. Willett, Acta Crystallogr. Sect. B, 44 (1988) 503.
10 R.D. Willett, J.A. Haugen, J. Lebsack and J. Morrey, Inorg. Chem., 13 (1974) 2510.
11 L. Antolini, G. Marcotrigiano, L. Menabue and G.C. Pellacani, J. Am. Chem. Soc., 102 (1980) 1303.
12 S. Brownstein, N.F. Han, E. Gabe and F. Lee, Can. J. Chem., 67 (1989) 551.
13 A.F. Wells, J. Chem. Soc., (1947) 1670.
14 L. Helmholz, J. Am. Chem. Soc., 69 (1947) 886.
15 A. Enberg, Acta Chem. Scand., 24 (1970) 3510.
16 A.W. Schlueter, R.A. Jacobson and R.E. Rundle, Inorg. Chem., 5 (1966) 277.
17 R.D. Willett and K. Chang, Inorg. Chim. Acta, 4 (1970) 447.
18 T. Li and G.D. Stucky, Inorg. Chem., 12 (1973) 441.
19 R.D. Willett and U. Geiser, Inorg. Chem., 25 (1986) 4558.
20 For a review, see C.P. Landee, A. Dijili, D.F. Mudgett, M. Newhall, H. Place, B. Scott and R.D. Willett, Inorg. Chem., 27 (1988) 620.
21 M.R. Bond and R.D. Willett, Acta Crystallogr. Sect. C, 43 (1987) 2304.
22 B. Scott and R.D. Willett, Inorg. Chim. Acta, 141 (1988) 193.
23 U. Geiser, R.D. Willett, M. Lindbeck and K. Emerson, J. Am. Chem. Soc., 108 (1986) 1173. M.R. Bond and R.D. Willett, Inorg. Chem., 28 (1989) 3267.
24 M.R. Bond, Ph.D. Thesis, Washington State University, 1990.
25 U. Geiser, R.M. Gaura, R.D. Willett and D.X. West, Inorg. Chem., 25 (1986) 4203.
26 See, for example, W.E. Marsh, W.E. Hatfield and D.J. Hodgson, Inorg. Chem., 27 (1988) 1819.
27 T. Manfridini, G.C. Pellacani, A. Bonamartini-Corradi, L.P. Battaglia, G.G.T. Guarini, J.G. Giusti, G. Pon and R.D. Willett, Inorg. Chem., 29 (1990) 2221.
28 M.R. Bond, G. Rubenacker and R.D. Willett, Inorg. Chem., 29 (1990) 2713.
29 T.E. Grigereit, B.L. Ramakrishna, H. Place, R.D. Willett, G.C. Pellacani, T. Manfredini, L. Menabue, A. Bonamartini-Corradi and L.P. Battaglia, Inorg. Chem., 26 (1987) 2235.
30 C.K. Prout and P.J. Murray-Rust, Chem. Soc. A, (1969) 1520.
31 J.W. Weenk and A.L. Spek, Cryst. Struct. Commun., 5 (1976) 805.
32 M.R. Bond and R.D. Willett, to be published.

33 W.G. Haije, J.A.L. Dobbelaar and W.J.A. Maaskant, Acta Crystallogr. Sect. C, 42 (1986) 1485.
34 R.E. Caputo, M.J. Vukosavovich and R.D. Willett, Acta Crystallogr. Sect. B, 32 (1976) 2516.
35 L. Antolini, L. Marcotrigiano, L. Menabue and G.C. Pellacani, J. Am. Chem. Soc., 102 (1980) 5506.
36 S.H. Simonsen and R.L. Harlow, Am. Crystallogr. Assoc. Ser., 2(1) (1977) 5, Abstract HN5.
37 L. Antolini, L. Menabue, G.C. Pellacani, M. Saladini, G. Marcotrigiano and W. Porzio, J. Chem. Soc. Dalton Trans., (1981) 1753.
38 K.B. Yatsimirskii, Yu.T. Struchkov, A.S. Batsanov and E.I. Sinyavskaya, Koord. Khim., 11 (1985) 826.
39 D.N. Anderson and R.D. Willett, Inorg. Chim. Acta, 8 (1974) 167.
40 R. Fletcher, J.J. Hansen, J. Livermore and R.D. Willett, Inorg. Chem., 22 (1983) 330.
41 K.E. Halvorson, T. Grigereit and R.D. Willett, Inorg. Chem., 26 (1987) 1716.
42 R.D. Willett, J. Coord. Chem., 19 (1988) 253.